Fine Structure of the Orion Proplyds:
Mass Loss, Shocks, Jets, and Binarity

W. J. Henney
Instituto de Astronomía, UNAM, Morelia

Contents

Credits

This talk draws directly on work carried in out in collaboration with the following people:

- Bob O'Dell (*Vanderbilt*)
- Jane Arthur, Fulgencio García-Arredondo, Teresa García-Díaz, Stan Kurtz (*Morelia*)
- John Meaburn, Simon Garrington, Matt Graham, Tim O'Brien (*Jodrell Bank*)

1. Introduction

1.1. What are the Proplyds?

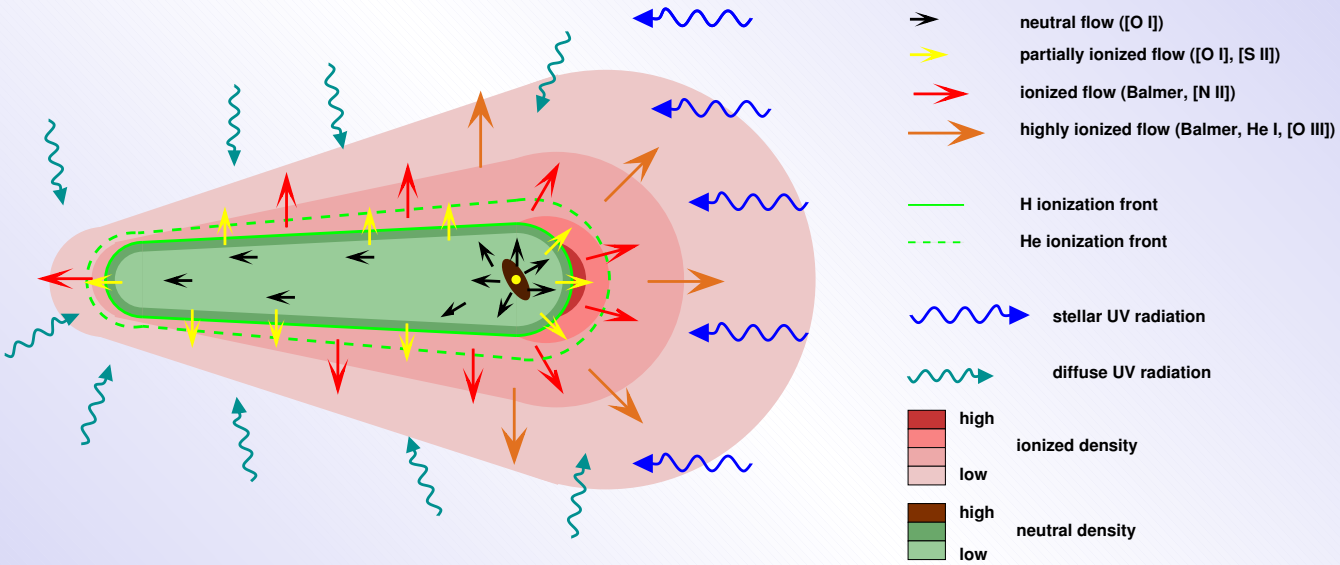

Components of the photoevaporating flow in a proplyd

- Accretion disks surrounding young low-mass stars, which are being photoevaporated by the ultraviolet radiation in their environment.
- The majority of known proplyds ($N \approx 100$) are found in the Orion nebula (M42) at a distance of 430 pc.

1.2. Comparison with Other Photoevaporation Flows

F_*: Ionizing flux	α: Recombination coefficient	n_0: Density at IF
c_0 : Sound speed (≈ 12 km s^{-1})	h: Flow thickness ($\approx 0.1 r_0$)	r_0 : IF radius ($\approx 10^{14}$ cm)

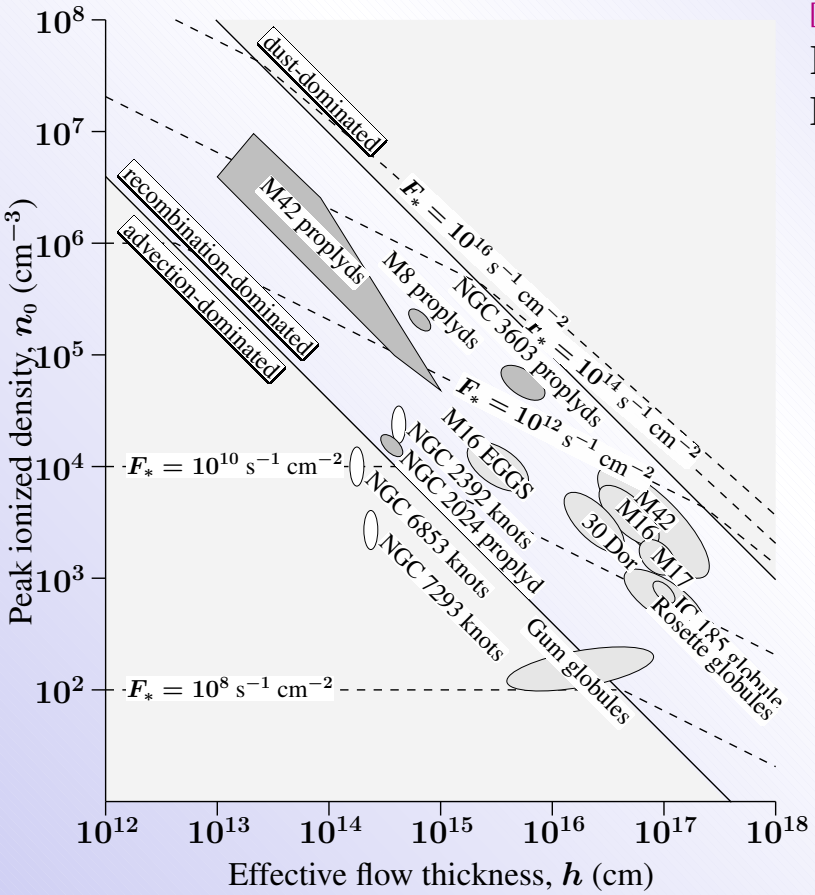

[Henney 2001 RevMexAA(SC) 10, 57]

Ionization balance for a D-critical front:

$$F_* \simeq c_0 n_0 + \alpha n_0^2 h$$

- If the first term on the RHS is negligible, the flow is *recombination dominated*
- Otherwise, the flow is *advection dominated*
- Most photoevaporation flows in H II regions fall along a recombination-dominated "main sequence" that spans at least 4 orders of magnitude in size and density, with $n_0 \sin h^{-1}$.
- The *ionization parameter*, $U \equiv F_*/(cn_0)$, is hence roughly constant for these flows at $U \approx 10^{-3}$.

1.3. Technicolor Proplyds and CKnots—Different Flow Regimes

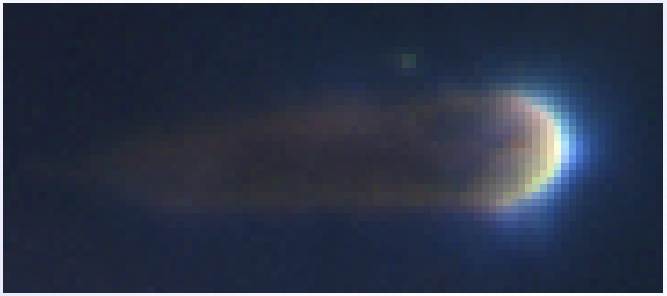

[N II] 6584Å Hα 6563Å [O III] 5007Å

- **Proplyds:** Red⟶Green⟶Blue
- Classical ionization stratification
- Recombination-dominated flow

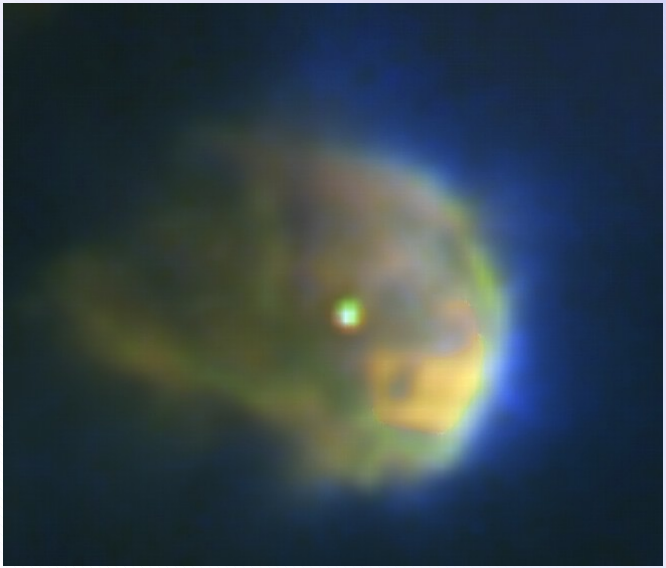

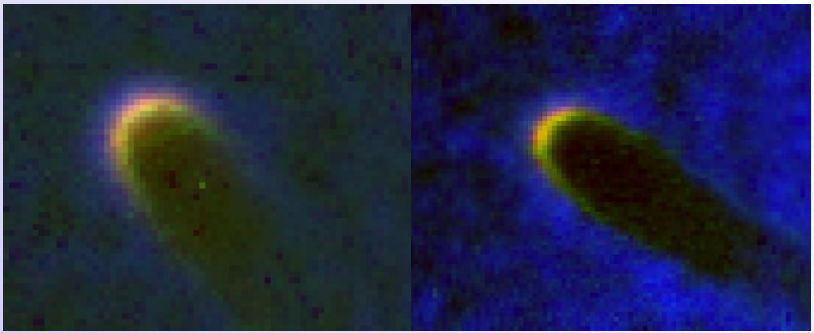

- **Helix CKnots:** Green⟶Red⟶Blue
- Thick IF: spatially resolved temperature gradients
  [O'Dell, Henney, & Burkert 2000]
- Advection-dominated flow
  [López-Martín et al. 2001]

2. Mass Loss Rates and Lifetimes

2.1. The Lifetime "Problem"

- The best studies indicate that

$$M < 0.01\ \mathrm{M}_\odot$$
$$\dot{M} > 10^{-7}\ \mathrm{M}_\odot\ \mathrm{yr}^{-1}$$

- $t_{\rm life} = M/\dot{M} \Rightarrow$ Proplyds should not survive longer than 10^5 years
- However, the stars in the Trapezium cluster have an average age of 10^6 years

Disk Masses:

- Calculated from continuum observations at mm wavelengths [Lada et al. 1996; Bally et al. 1998b].
- Results: $M = 0.007$–$0.02\ \mathrm{M}_\odot$ for larger disks, $M < 0.005\ \mathrm{M}_\odot$ for most bright proplyds.
- Caveat: these masses depend on assumptions about the mm-wave grain opacity—if grains have grown substantially in the disk [Throop et al. 2001] then masses may be higher.

Mass Loss Rate:

$$\dot{M} = \int_{\rm S} \text{density} \times \text{velocity}\ dA$$

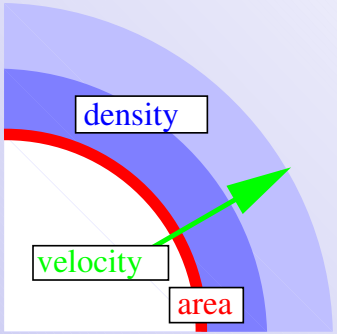

	Early Work	Recent Work
Density:	Hα surface brightness	NUV C III doublet
Velocity:	Assumed $\approx c_0$	Optical spectroscopy

2.2. Early Work on $\dot{M}$

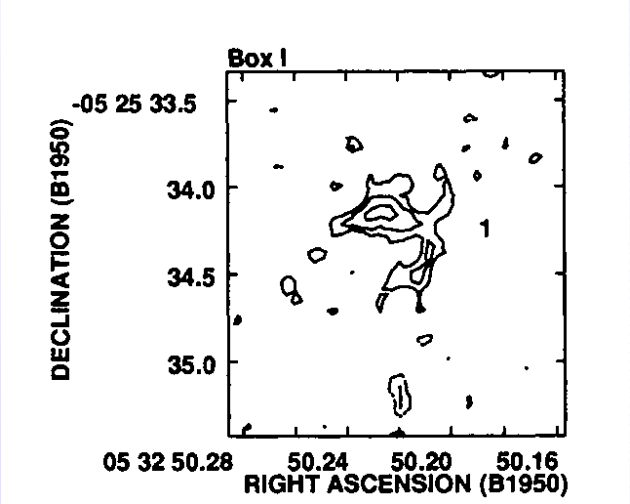

[Churchwell 1987]

- Radio-continuum observations
- The first to suggest the correct model for the proplyds
- "Back-of-envelope" calculation
- Result: $\dot{M} \simeq 10^{-6}$ M$_\odot$ yr^{-1}

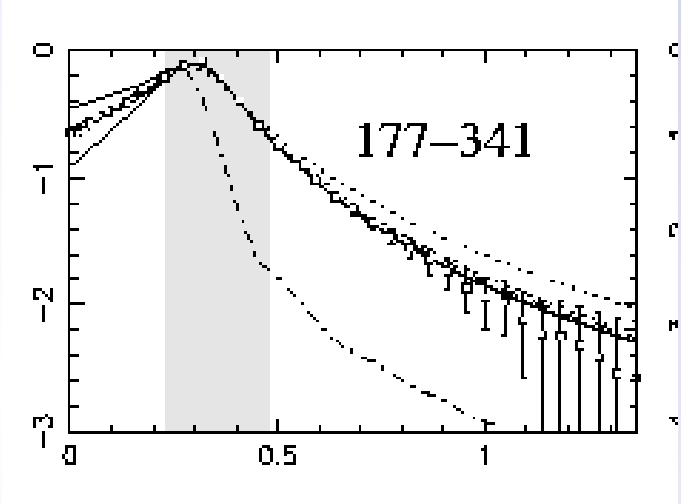

[Henney & Arthur 1998, AJ 116, 322]

- Model fits to the proplyd heads
- Density determined from Hα emission (uncertainties due to dust extinction)
- Invented velocities
- Result: $\dot{M} \simeq 10^{-7}$–10^{-6} M$_\odot$ yr^{-1}

[Henney & O'Dell 1999, AJ 118, 2350]

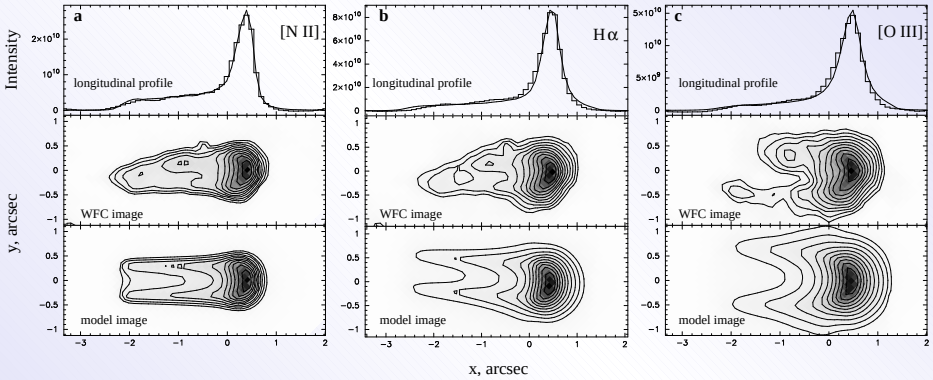

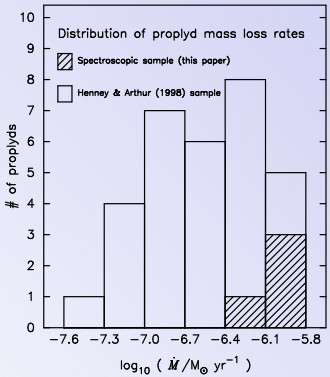

- Extends [Henney & Arthur 1998] models to include the tails
- Flow velocity found via ground-based optical spectroscopy
- Confirms supposition of D-critical IF
- Clear evidence for acceleration of photoevaporation flow

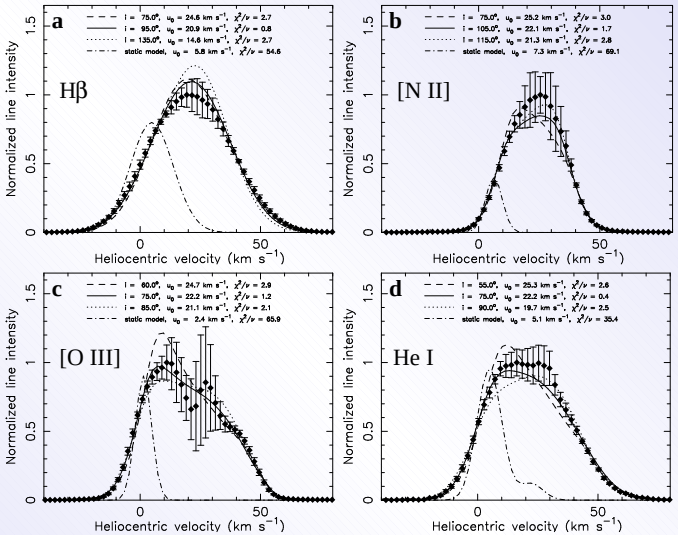

2.3. STIS Spectroscopy of 167–317

[Henney, O'Dell, Meaburn, Garrington, & López, 2001, ApJ submitted]

Instrument: STIS NUV-MAMA, E230H

Velocity Resolution: $\sim$2.5 km s^{-1}

Angular Resolution: $\sim$30 mas (15AU@430pc)

Observed Lines: [C III] 1906.68 Å, C III] 1908.73 Å

Slit Dimensions: $6'' \times 0.2''$

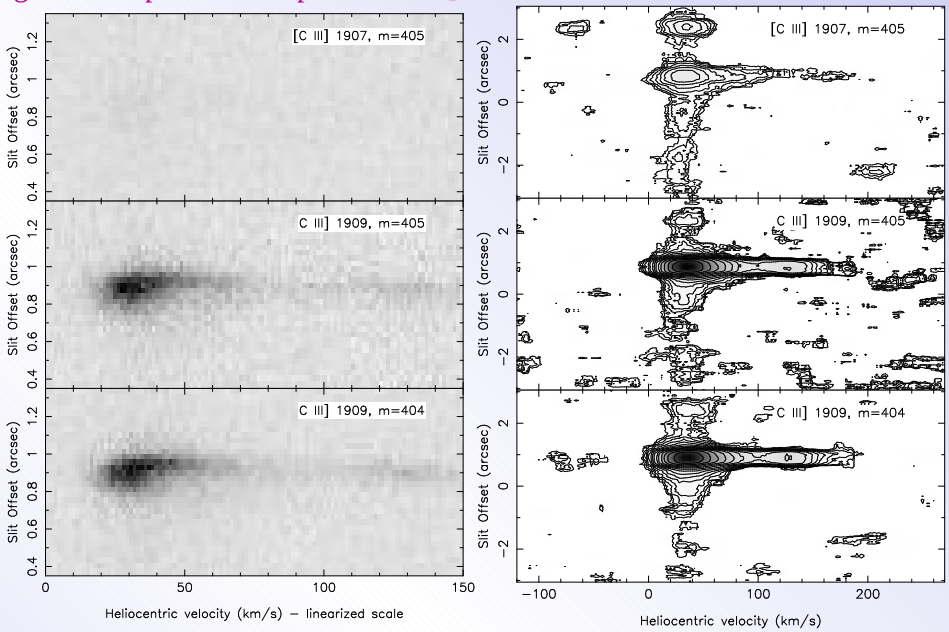

Motivation:

- Kinematic test of photoevaporation models free from nebular background problems

Complications:

- Intrinsically weak lines + short wavelength + very small pixels + "fragile" detector = low S/N
- Data reduction non-trivial due to order overlap

2.3.1. Improved Photoevaporation Model

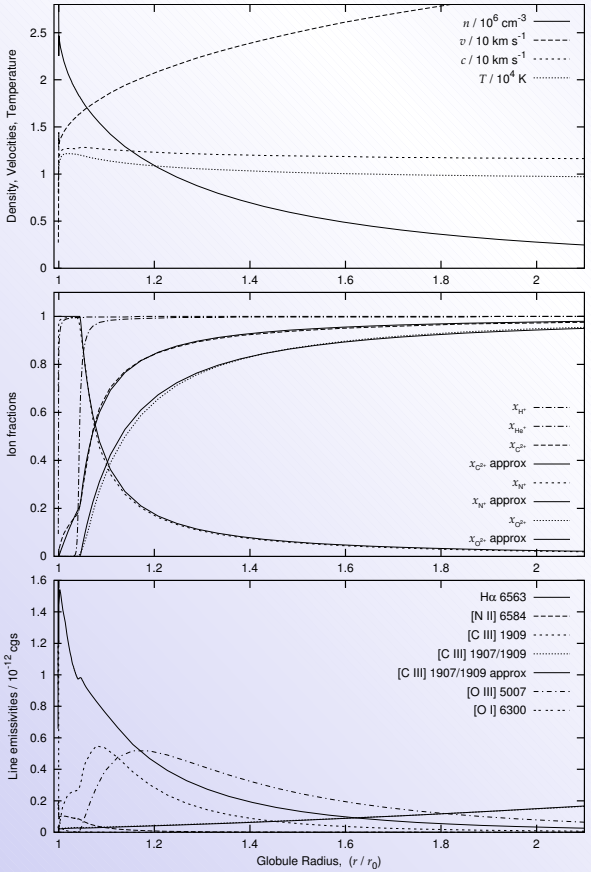

- Radiative transfer of direct and diffuse ionizing continua of H and He
- Ad hoc shape for inner boundary (Hydrogen IF)
- Ionization of all other elements calculated self-consistently
- Calibrated with the photoionization code Cloudy

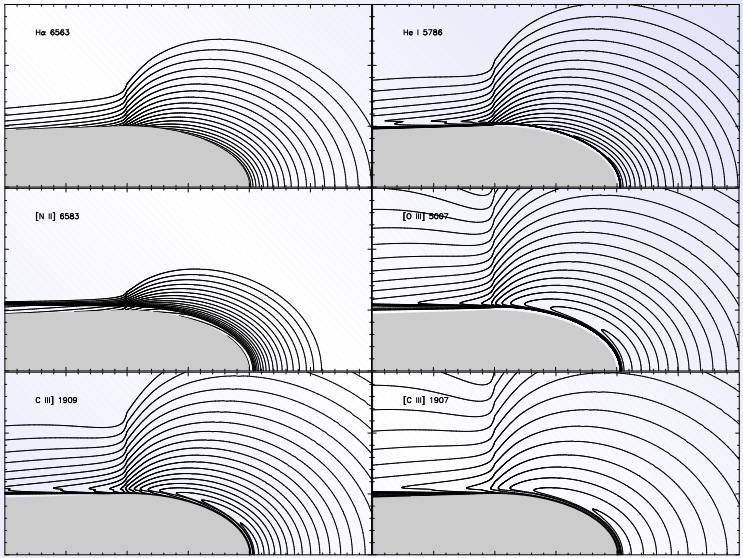

2.3.2. Results of Model Fits to STIS Data

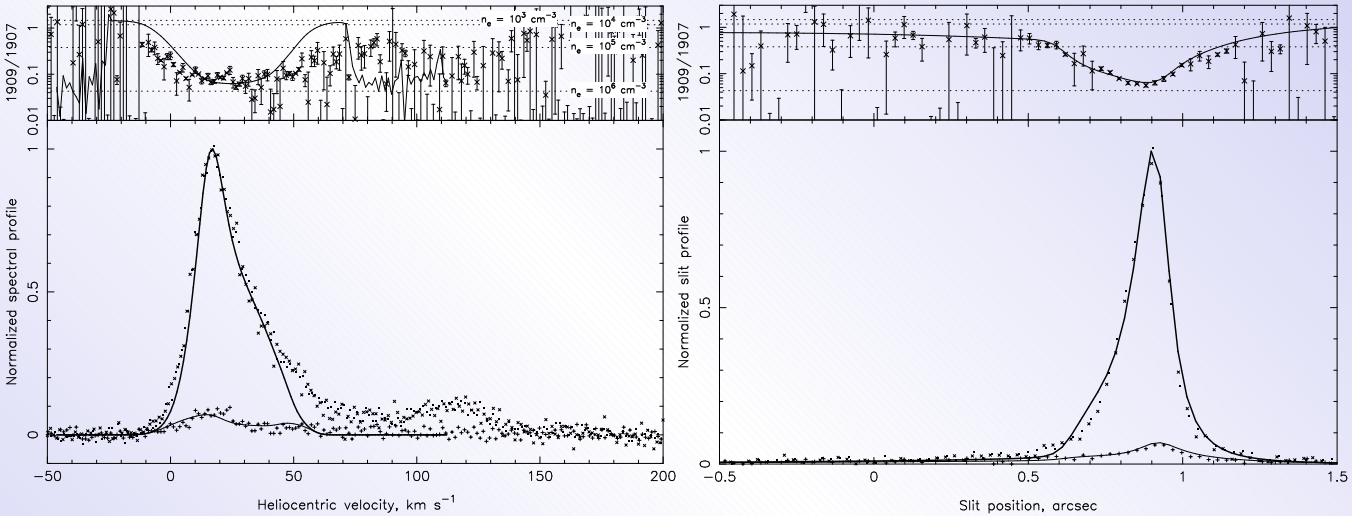

- A model fitted only to the *HST* images well reproduces the C III spectral and spatial profiles
- It also provides a good fit to the electron density as determined from the doublet ratio
- Result: $\dot{M} \simeq 10^{-6}$ M$_\odot$ yr^{-1}—*Same as Churchwell (1987)!*

2.3.3. Implications of Short Proplyd Lifetimes

It now seems inescapable that

proplyd evaporation times $\ll$ stellar ages.

Attempts to explain this fall into two categories:

Just passing through…

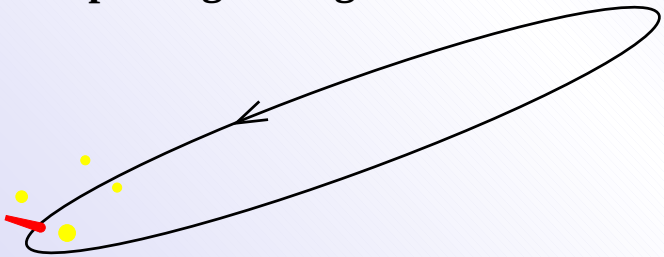

- Proplyds are on more-or-less radial orbits and only spend a short time close to the ionizing star [Hollenbach & Störzer 1999].
- More recent stellar dynamic calculations [Scally & Clarke 2001] seem to rule this out.

Young H II region

- Requires the ionizing stars to be much younger than the majority of low-mass stars in the Orion Nebula Cluster
- Somewhat plausible since the birth of a massive star may “switch off” subsequent star formation in its vicinity
- Direct evidence of extreme youth ($< 10^5$ years) for at least one of the Trapezium OB stars [Palla & Stahler 2001]

3. Standoff Bowshocks: Wind-Wind Collisions

[García-Arredondo, Henney, & Arthur 2001, ApJ in press]

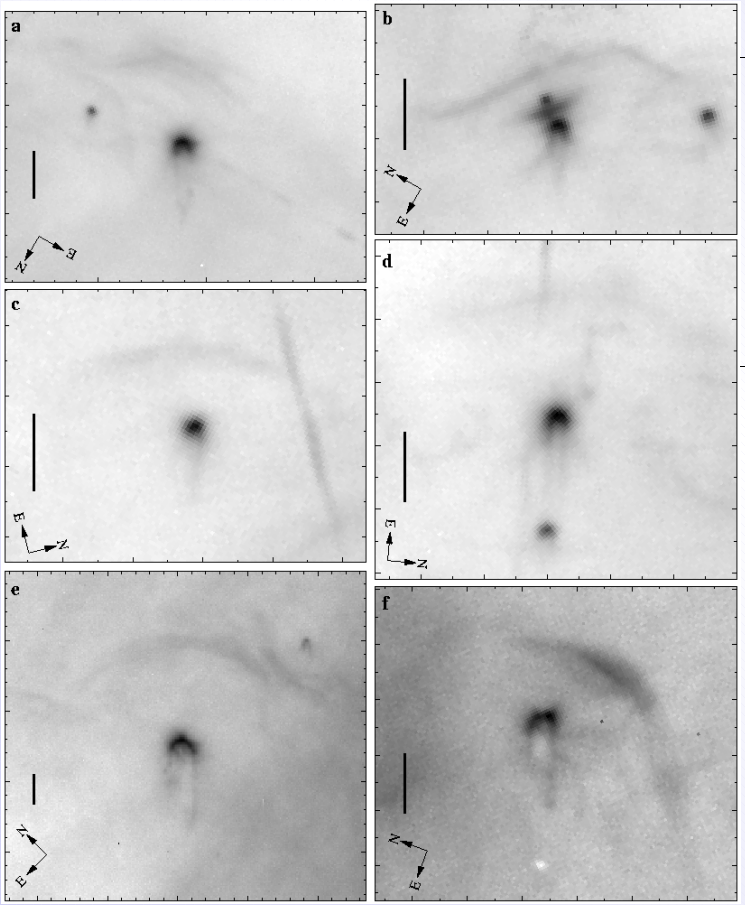

Proplyd	D sin i 10^{16}	$R_{\rm shock}$ 10^{14}	$R_{\rm IF}$ 10^{14}	n_0 10^6 cm^{-3}
158–323	6.08	116.0	6.3 ± 0.6	2.33 ± 0.22
161–324	3.90	66.0	3.5 ± 0.3	4.13 ± 0.23
163–317	4.46	144.0	5.0 ± 0.6	3.13 ± 0.30
163–323	1.34	25:	2.2 ± 0.6	10.0 ± 2.0
166–316	4.52	40.0	2.5 ± 0.6	4.13 ± 0.16
167–317	5.05	116.0	7.9 ± 0.3	2.60 ± 0.11
168–326E	4.26	74.0	6.3 ± 0.6	2.33 ± 0.04
168–328	4.28	65.0	2.8 ± 0.3	4.00 ± 0.01
177–341	16.67	258.0	20.4 ± 1.6	0.41 ± 0.02
180–331	16.20	97.0	12.2 ± 1.2	0.48 ± 0.03

- Most of the proplyds closer to θ^1C Ori show high-ionization emission arcs, displaced $\approx 1''$ towards the ionizing star

  [Bally et al. 1998]

- These are believed to be due to the interaction of the proplyd photoevaporation flow with the stellar wind from θ^1C Ori

  [Johnstone et al. 1998]

3.1. Location of the Bowshocks

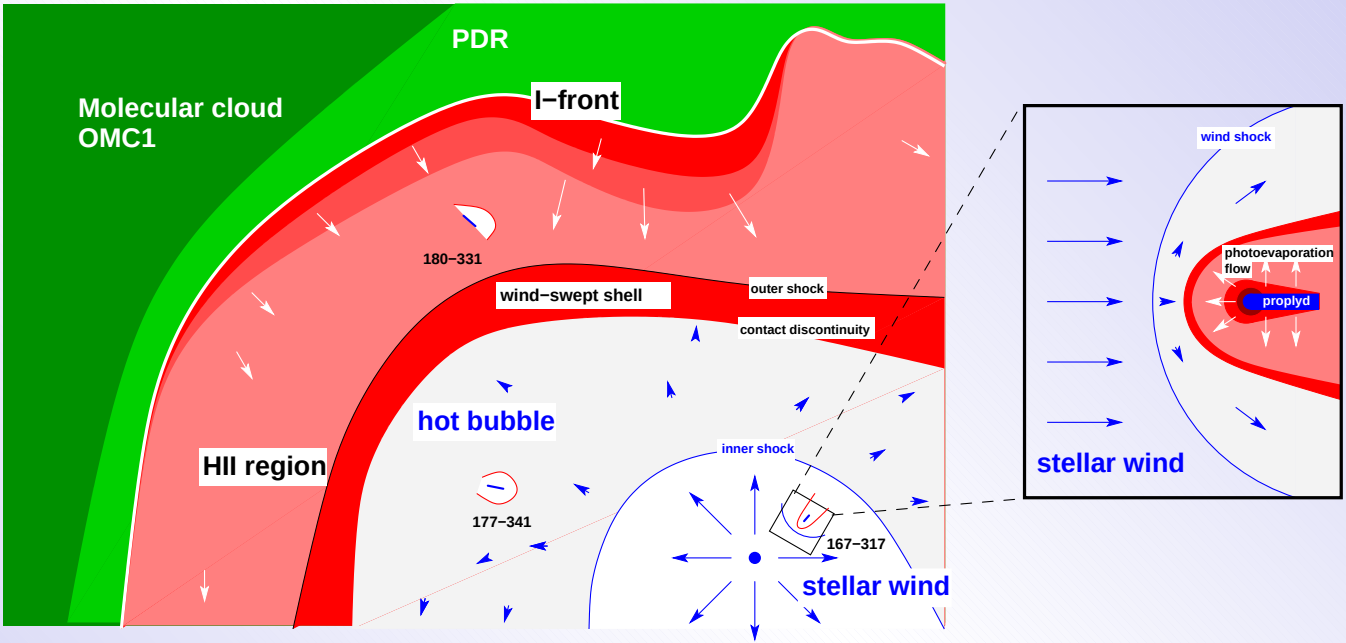

In principle, the proplyds may lie in 1 of 3 regions:

1. In the fast supersonic stellar wind
2. In the hot shocked subsonic wind bubble
3. Outside the domain of influence of the stellar wind, inside the photoevaporation flow from the nebula's principal IF

3.2. Ram Pressure Balance

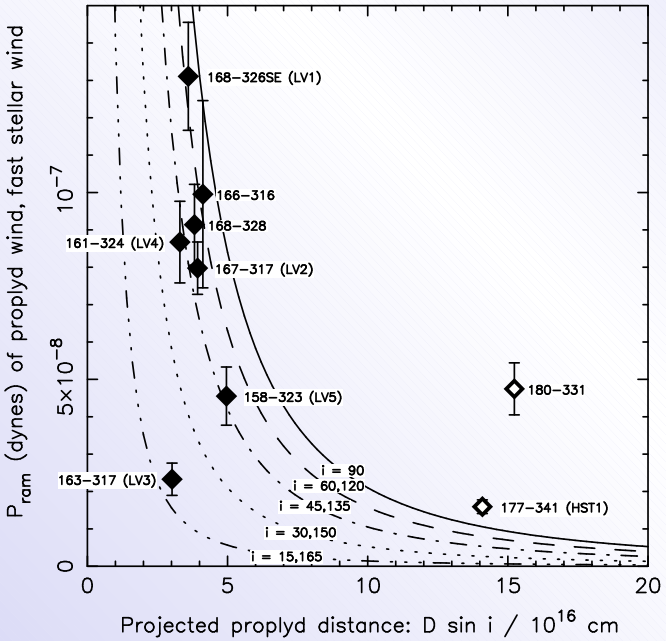

Ram pressure of the proplyd photoevaporated flows (diamonds) and supersonic stellar wind (lines). The value of $\dot{M}_{\rm w} V_{\rm w}$ is chosen so that the proplyd LV2 (167–317) has an inclination angle $i = 50°$. Error bars are 1σ and represent the uncertainty in the observed parameters of the proplyd flows.

Ram pressure of proplyd flow at bowshock:

$$P_{\rm pf} = 1.67 \times 10^{-6}\, \mathcal{M}_{\rm s}\, (R_{\rm IF}/R_{\rm s})^2\, n_6\, c_{10}^2.$$

Ram pressure of stellar wind:

$$P_{\rm sw} = 5.0 \times 10^{-7}\, \dot{M}_{-7}\, V_3\, D_{16}^{-2}.$$

For the inner proplyds, these pressures are in balance if one assumes stellar wind aprameters of

$$\dot{M}_{\rm w} = 3.5 \times 10^{-7}\, {\rm M}_\odot\ {\rm yr}^{-1}$$
$$V_{\rm w} = 1200\ {\rm km\ s}^{-1}$$

For further proplyds, this is no longer true: perhaps they lie in the shocked subsonic wind bubble.

3.3. Numerical Simulations

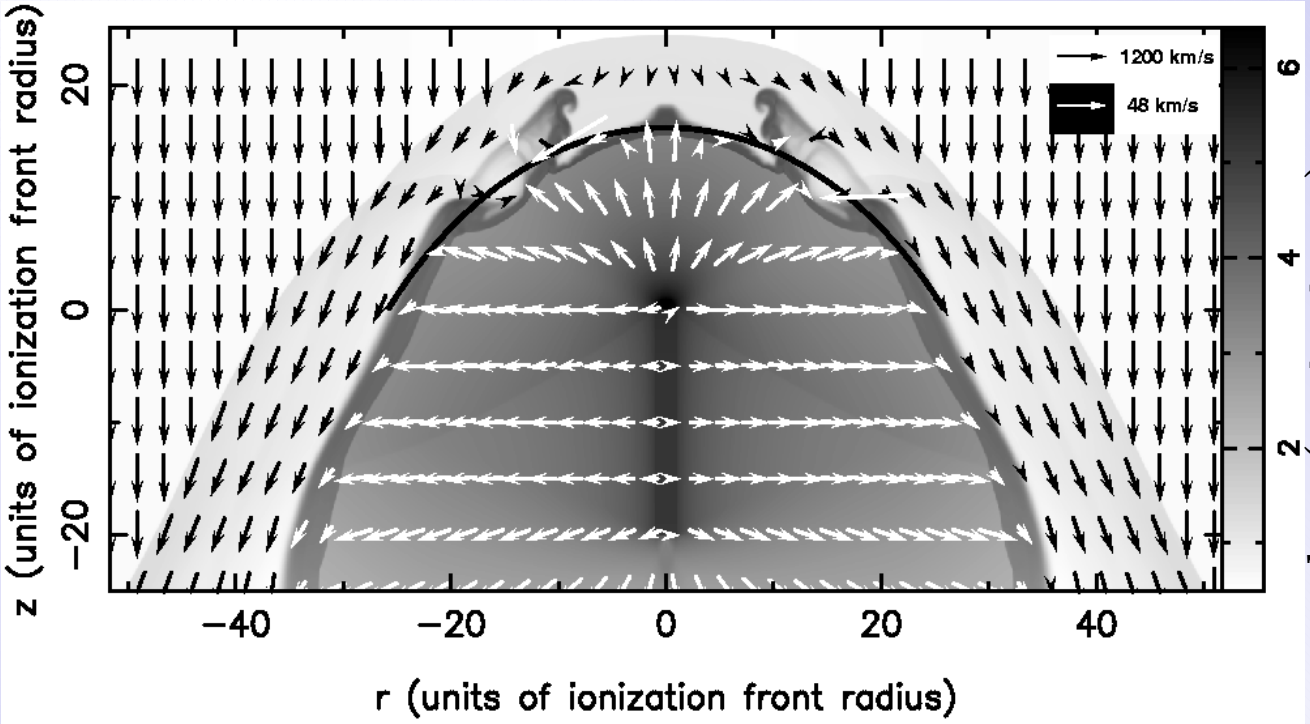

- Simulations of the case of a supersonic stellar wind produce good agreement with the observed morphology of the bowshocks.
- The bowshock shape is similar to the momentum-conserving thin-shell solution [Cantó, Raga & Wilkin 1996], except for some corrugation, which is probably due to Kelvin-Helmholtz instabilities.

3.3.1. Optical Line Emission

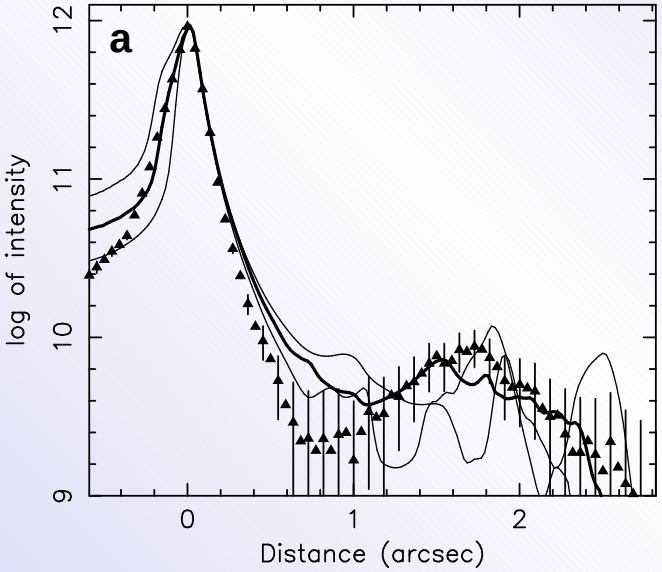

- The relative surface brightness of the 167–317 bowshock in Hα is well-reproduced assuming a pure photoionization spectrum at $\approx 10^4$ K
- The favored inclination is consistent with that found from the STIS spectroscopy
- There is slight evidence that the visual dust opacity in the photoevaporation flow is lower than "normal"

3.3.2. MIR Dust Emission

Map of hydrogen column density of the Case 1 simulation, smoothed by a Gaussian of FWHM 0.5″ for comparison with mid-infrared observations [Hayward, Houck, & Miles 1994]

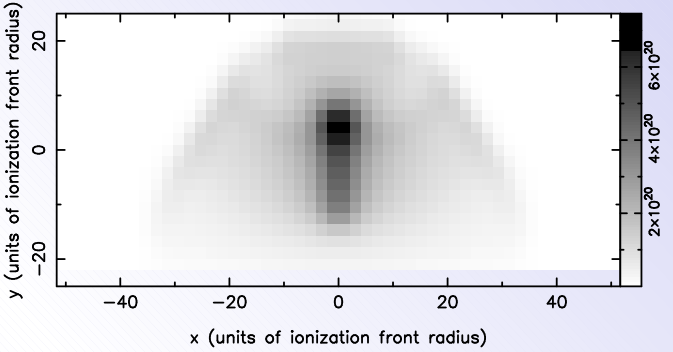

- We require either
  1. MIR dust opacity <10% of the "standard" value, or
  2. $T_{\rm d} \ll 200$ K $\Rightarrow a > 1$ μm
- We also find that $T_{\rm d}$ must be slightly lower in the base of the ionized photoevaporation flow than in the standoff shocks. This is readily explained by the increasing attenuation of the ionizing radiation field as one approaches the proplyd IF [Baldwin et al. 1991]

3.3.3. The Subsonic Case

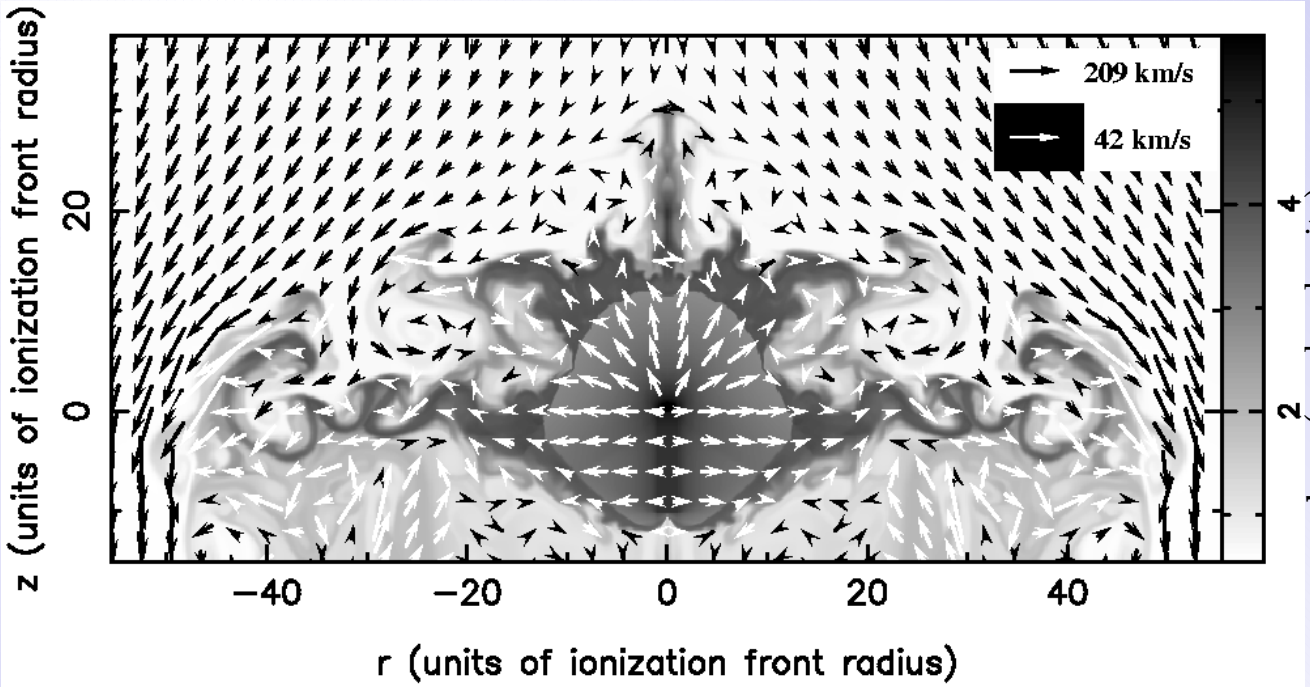

- Simulations of a proplyd immersed in the hot shocked wind bubble fail to produce anything that looks like the observations!
- A thick shocked layer develops al around the proplyd, which is slowly entrained by the subsonic flow in the bubble, forming large filamentary vortices
- Problems are ameliorated if Mach number in bubble is higher

$\Rightarrow$ mass loading?

4. The Case Against Non-Thermal Emission

[Henney, García-Díaz, & Kurtz 2001, RevMexSC 10, 213]

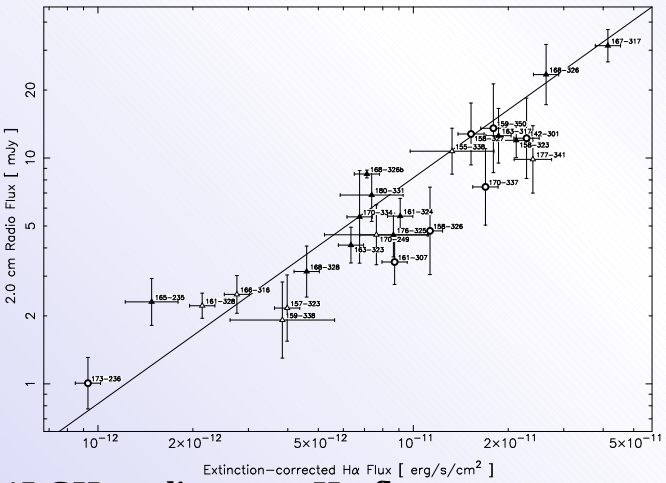

15 GHz radio versus Hα flux.

Previous classifications [Felli et al. 1993]:
○ nonthermal; ▲ thermal; △ uncertain
Line shows expected relation for optically thin free-free emission
Non-thermal emitters should have 15 GHz flux *above* the line

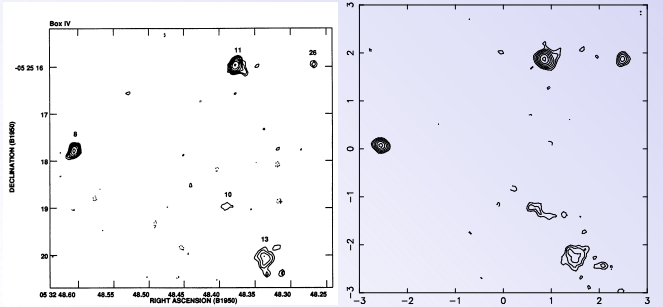

Real map ..... Fake map

- Reanalysis of archival radio observations of the proplyds fails to show any evidence for non-thermal emission
- Previous claims of temporal variability seem to be an observational artifact since they vary below the thermal line (tip-of-the-iceberg effect)
- Spectra from 1.5 to 86 Ghz are also consistent with pure thermal emission.

5. Proplyd Jets

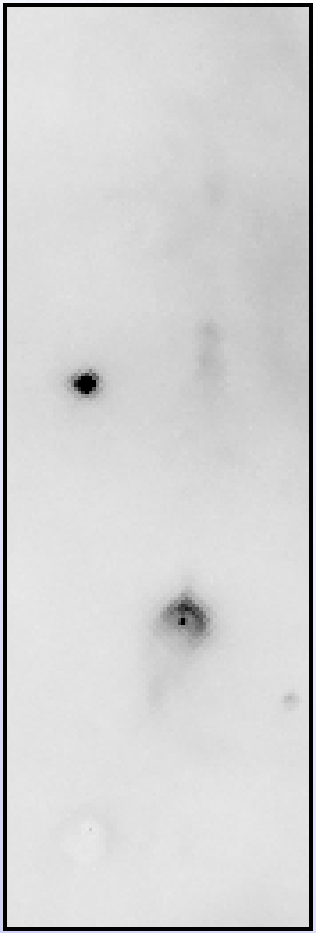

170–337 jet

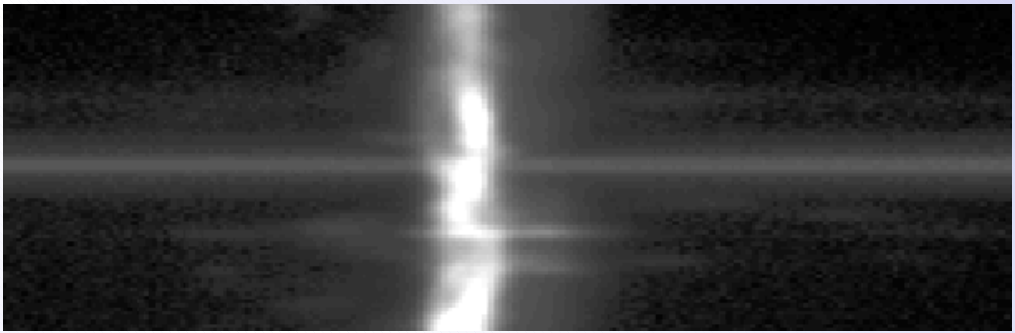

- High-speed flows from the proplyds have long been recognised spectroscopically [Meaburn 1988]
- However, their identification as *jets* had always been tentative [Meaburn et al. 1993; Massey & Meaburn 1995] . . .
- . . . and some spectacularly misguided models had emerged [Henney et al. 1997] . . .
- . . . until *HST* imaging [O'Dell 1998] showed that they were all jets after all
- Scores of them are now known [Bally, O'Dell, & McCaughrean 2000]
- Tendency to be one-sided, as with jets in other ionized regions [Bally & Reipurth 2000]

5.1. The 167–317 Jet: A Case Study

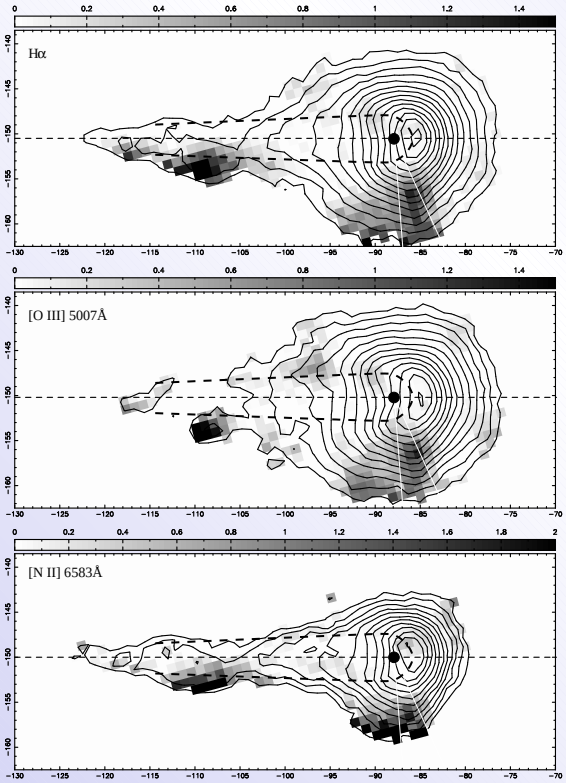

[Henney et al. 2001]

- Appears to be one-side at its base close to the IF
- Further-out filaments are more symmetric—some evidence for interaction with bowshock of binary companion

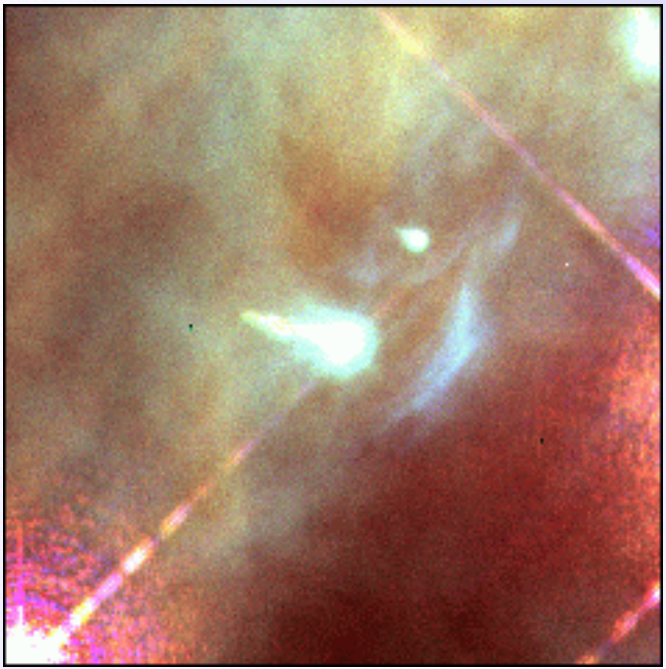

5.1.1. Spectroscopy of the 167–317 Jet

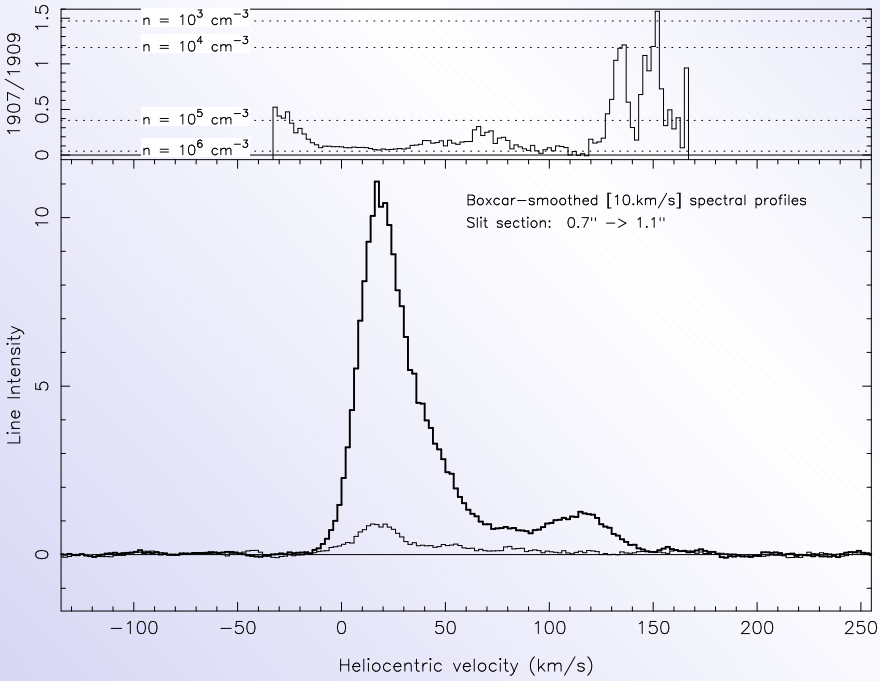

- C III] and [O III] profiles show jet redshift of $\approx 100\ \mathrm{km\ s^{-1}}$ with respect to the systemic velocity
- C III doublet ratio indicates $n_e \approx 10^6\ \mathrm{cm^{-3}}$ at base of jet—very similar to density in proplyd photoevaporation flow
- A Simple conical jet model gives the following parameters:
  - inclination: $i_j > 135°$
  - opening angle: $\theta_j < 5°$
  - mass loss rate: $\dot{M}_j \simeq 10^{-8} \left|\cos i_j\right| \mathrm{M_\odot\ yr^{-1}}$.

5.1.2. Radio Emission from the 167–317 Jet

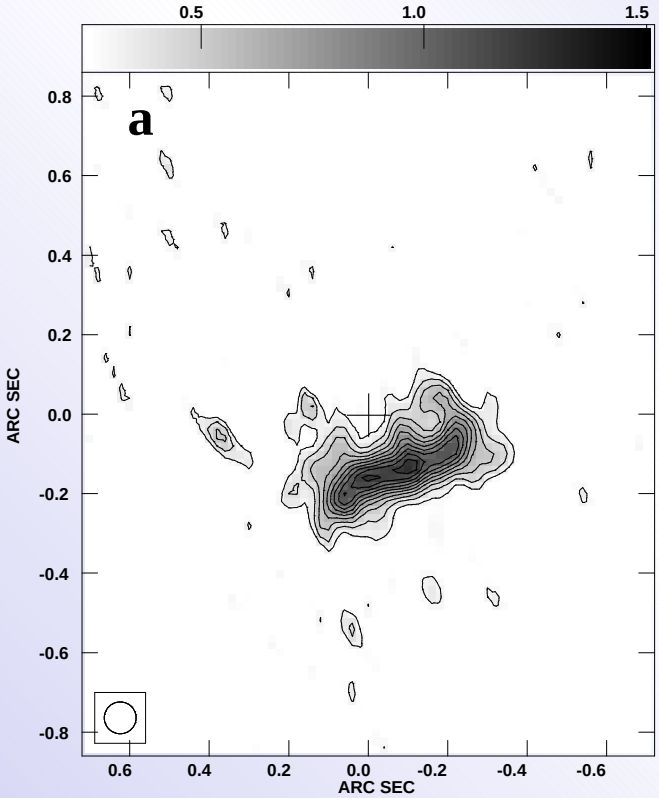

Observed 6 cm MERLIN image

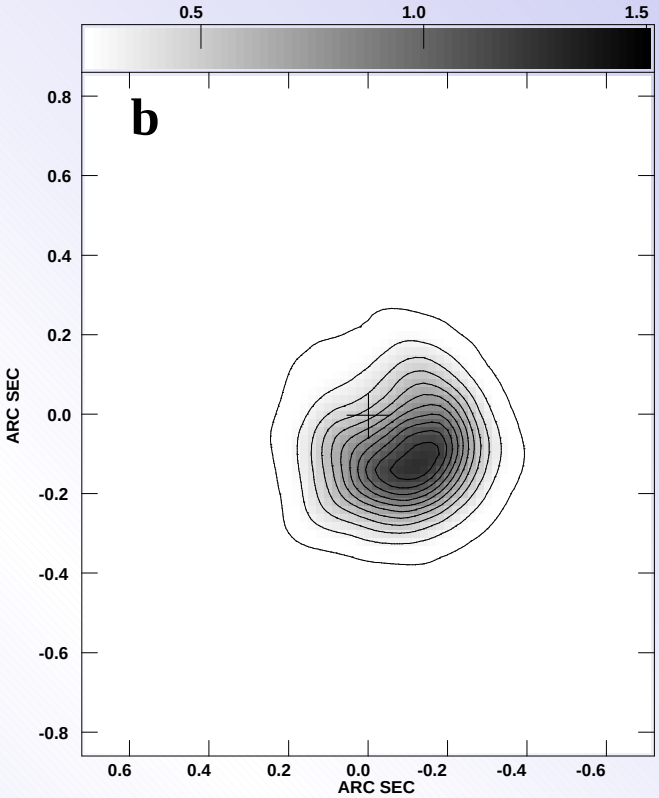

6 cm image predicted from Hα surface brightness

- There are interesting differences between the radio emission from the jet and that expected due to thermal emission
- Could it be non-thermal afer all?

6. 168–326: An Interacting Proplyd Binary

[Henney 2001, in prep; Graham, Meaburn, Garrington, O'Brien, Henney, & O'Dell 2001, in prep]

6.1. Colliding Proplyd Flows

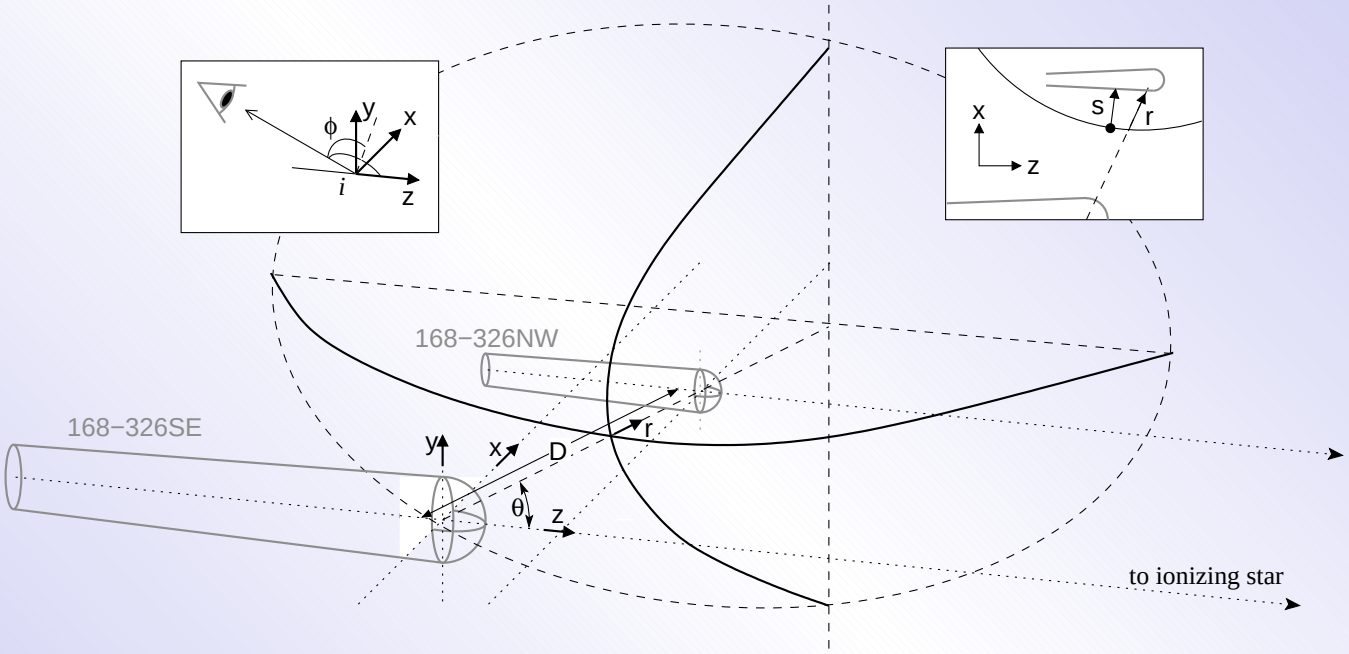

- The photoevaporation flows from each proplyd collide at mildly supersonic velocities, forming a dense interaction shell bounded by two weak shocks
- The resulting bowshock structure will have a complicated asymmetrical shape

6.2. Shape of the Shocked Shell

- A ram-pressure balance calculation can give the approximate shape of the shell …
- …but this ignores centrifugal forces—need to adapt technique of [Cantó, Raga, & Wilkin 1996]
- Meanwhile, can use an approximate 2d treatment:

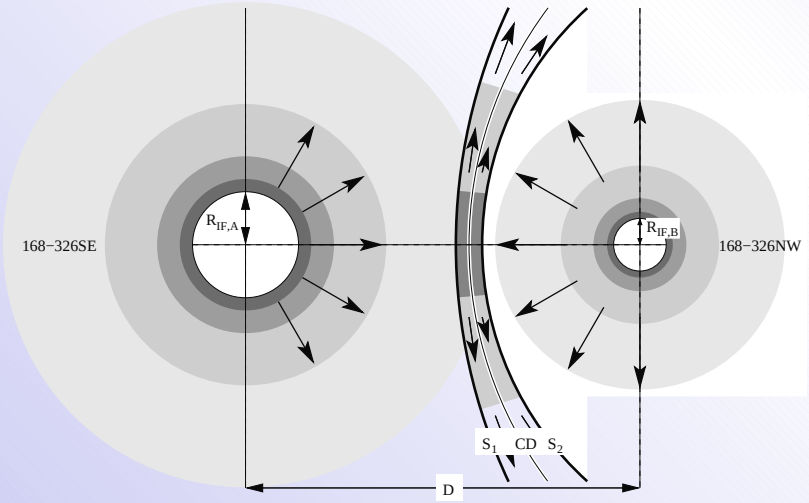

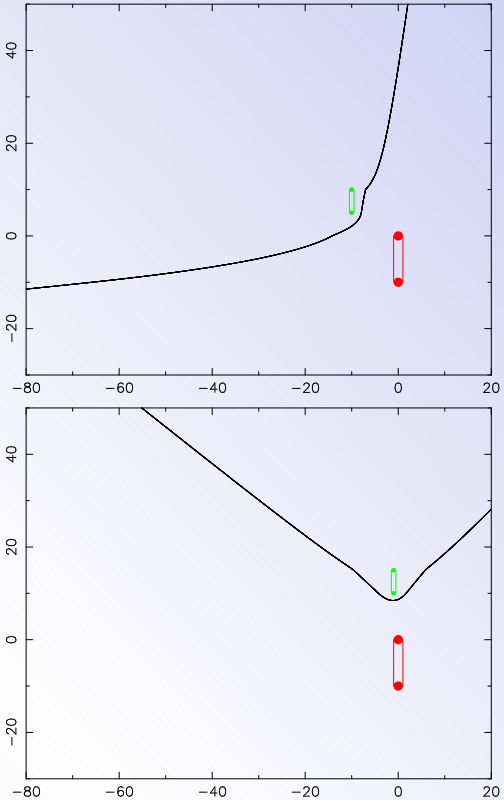

- Wings of the bowshock will eventually interact with the stellar wind from θ^1C Ori …

6.3. Constraining the Geometry

…deforming the standoff shock:

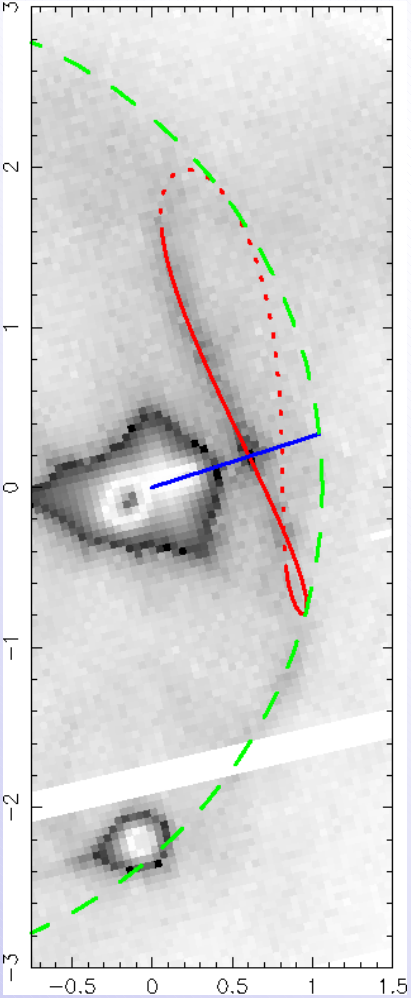

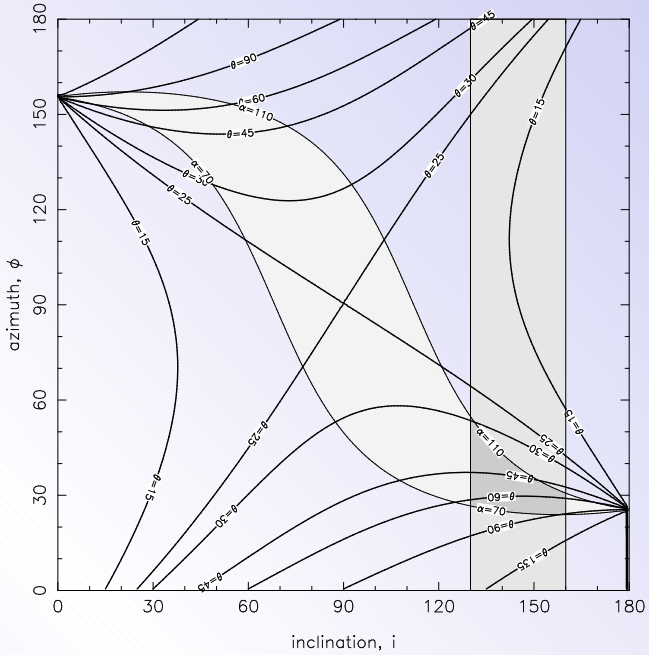

The 3 angles, θ, i, ϕ, that characterize the system are constrained by observations of

- kinematic profile
- relative projected proplyd positions
- apparent perpendicular elongation of bowshock nose

The preferred solution is

$$\theta \approx 90°, i \approx 150°, \phi \approx 25°$$

6.4. Excess Radio Emission

- As in the case of 167–317, the radio emission is puzzling
- At 6 cm the shock is brighter than the smaller proplyd, the opposite of what is seen in Hα
- Higher temperatures do not seem to be the answer since the cooling distance behind the shock is so short

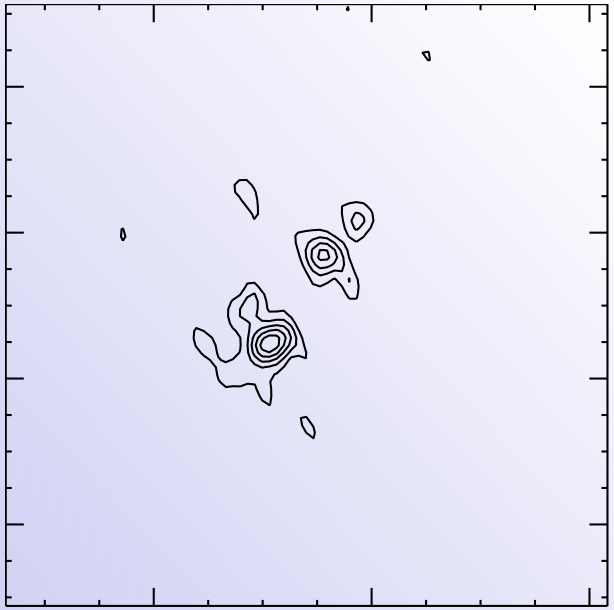

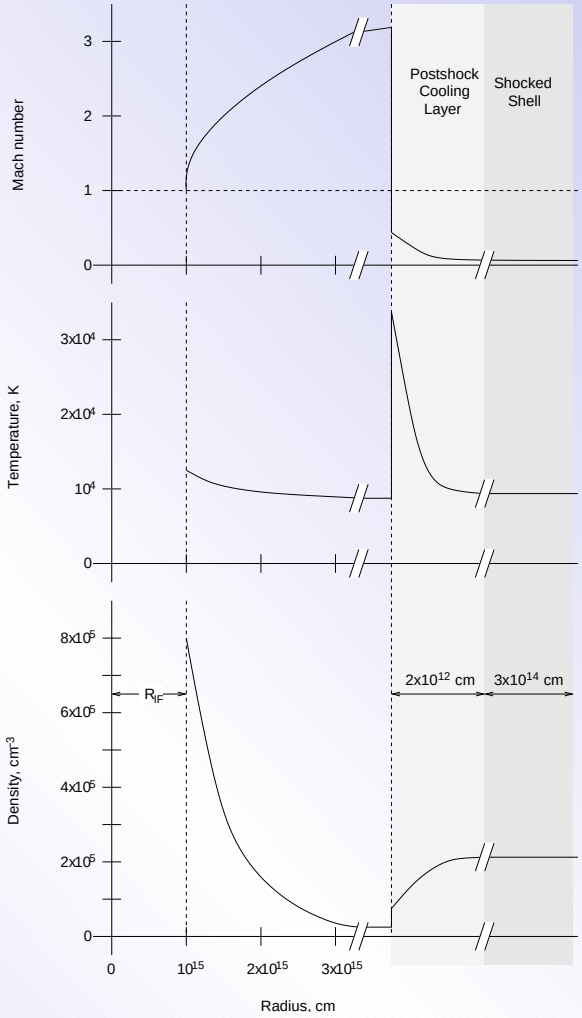

The End